

isotherm (15-16). Experimental  $q$ - $p$  isothermal data can be fitted to (15-19) by a nonlinear curve fit or by converting (15-19) to the following linear form, and using a graphical method or a linear-regression program to obtain  $k$  and  $n$ ;

$$\log q = \log k + (1/n)\log p \quad (15-20)$$

In the graphical method, data are plotted as  $\log q$  versus  $\log p$ ; the best straight line through the data has a slope of  $(1/n)$  and an intercept of  $\log k$ . In general,  $k$  decreases, while  $n$  increases with increasing temperature, approaching a value of 1 at high temperatures. Although (15-19) is empirical, it can be derived by assuming a heterogeneous surface with a nonuniform distribution of heat of adsorption (Brunauer [21]).

### Langmuir Isotherm

The Langmuir equation [28] is restricted to Type I isotherms. It is derived from mass-action kinetics, assuming that chemisorption is the reaction. Let the surface of the pores of the adsorbent be homogeneous ( $\Delta H_{\text{ads}} = \text{constant}$ ), with negligible interaction forces between adsorbed molecules. If  $\theta$  is the fraction of surface covered by adsorbed molecules,  $(1 - \theta)$  is the fraction of bare surface, and the net rate of adsorption is the difference between the rate of adsorption on the bare surface and the rate of desorption on the covered surface:

$$dq/dt = k_a p(1 - \theta) - k_d \theta \quad (15-21)$$

where  $k_a$  and  $k_d$  are the adsorption and desorption kinetic constants. At equilibrium,  $dq/dt = 0$  and (15-21) reduces to

$$\theta = \frac{Kp}{1 + Kp} \quad (15-22)$$

where  $K = k_a/k_d$  is the adsorption-equilibrium constant and

$$\theta = q/q_m \quad (15-23)$$

where  $q_m$  is the maximum loading corresponding to complete surface coverage. Thus, the Langmuir adsorption isotherm is restricted to a monomolecular layer. Combining (15-23) with (15-22) results in the *Langmuir isotherm*:

$$q = \frac{Kq_m p}{1 + Kp} \quad (15-24)$$

At low pressures, if  $Kp \ll 1$ , (15-24) reduces to the linear isotherm, (15-16), while at high pressures where  $Kp \gg 1$ ,  $q = q_m$ . At intermediate pressures, (15-24) is nonlinear in pressure. Although originally devised by Langmuir for chemisorption, (15-24) is widely applied to physical-adsorption data.

In (15-24),  $K$  and  $q_m$  are treated as constants obtained by fitting the nonlinear equation to experimental data or by employing the following linearized form, numerically or graphically:

$$\frac{p}{q} = \frac{1}{q_m K} + \frac{p}{q_m} \quad (15-25)$$

Using (15-25), the best straight line is drawn through a plot of points  $p/q$  versus  $p$ , giving a slope of  $(1/q_m)$  and an intercept of  $1/(q_m K)$ . Theoretically,  $K$  should change rapidly with temperature but  $q_m$  should not, because it is related through  $v_m$  by (15-7) to  $S_g$ . The Langmuir isotherm predicts an asymptotic limit for  $q$  at high pressure, whereas the Freundlich isotherm does not, as shown e.g. by the curve for Columbia G activated carbon in Figure 15.11.

### Other Adsorption Isotherms

Valenzuela and Myers [23] fit isothermal, pure-gas adsorption data to the three-parameter isotherms of Toth:

$$q = \frac{mp}{(b + p^t)^{1/t}} \quad (15-26)$$

where  $m$ ,  $b$ , and  $t$  are constants for a given adsorbate-adsorbent system and temperature.

Honig and Reyerson devised the three-constant UNILAN equation:

$$q = \frac{n}{2s} \ln \left[ \frac{c + pe^s}{c + pe^{-s}} \right] \quad (15-27)$$

where  $n$ ,  $s$ , and  $c$  are the constants for a given system and temperature. The Toth and UNILAN isotherms reduce to the Langmuir isotherm for  $t = 1$  and  $s = 0$ , respectively.

### EXAMPLE 15.4 Freundlich and Langmuir Isotherms.

Data for the equilibrium adsorption of pure methane gas on activated carbon (PCB from Calgon Corp.) at 296 K were obtained by Ritter and Yang [*Ind. Eng. Chem. Res.*, **26**, 1679–1686 (1987)]:

$q$ , cm <sup>3</sup> (STP) of CH <sub>4</sub> /g carbon	45.5	91.5	113	121	125	126	126
$P = p$ , psia	40	165	350	545	760	910	970

Fit the data to: (a) the Freundlich isotherm, and (b) the Langmuir isotherm. Which isotherm provides a better fit? Do the data give a reasonable fit to the linear isotherm?

### Solution

Using the linearized forms of the isotherm equations, a spreadsheet or other program can be used to do a linear regression:

(a) Using (15-20),  $\log k = 1.213$ ,  $k = 16.34$ ,  $1/n = 0.3101$ , and  $n = 3.225$ . Thus, the Freundlich equation is:

$$q = 16.34p^{0.3101}$$

(b) Using (15-25),  $1/q_m = 0.007301$ ,  $q_m = 137.0$ ,  $1/(q_m K) = 0.5682$ , and  $K = 0.01285$ . Thus, the Langmuir equation is

$$q = \frac{1.760p}{1 + 0.01285p}$$

The predicted values of  $q$  from the two isotherms are:

$p$ , psia	$q$ , cm <sup>3</sup> (STP) of CH <sub>4</sub> /g carbon		
	Experimental	Freundlich	Langmuir
40	45.5	51.3	46.5
165	91.5	79.6	93.1
350	113	101	112
545	121	115	120
760	125	128	124
910	126	135	126
970	126	138	127

The Langmuir isotherm fits the data significantly better than the Freundlich. Average percent deviations, in  $q$ , are 1.01% and 8.64%, respectively. One reason for the better Langmuir fit is the trend to an asymptotic value for  $q$  at the highest pressures. Clearly, the data do not fit a linear isotherm well at all.

### §15.2.2 Gas Mixtures and Extended Isotherms

Commercial applications of physical adsorption involve mixtures rather than pure gases. If adsorption of all components except one (A) is negligible, then adsorption of A is estimated from its pure-gas-adsorption isotherm using the partial pressure of A in the mixture. If adsorption of two or more components in the mixture is significant, the situation is complicated. Experimental data show that one component can increase, decrease, or have no influence on adsorption of another, depending on interactions of adsorbed molecules. A simple theoretical treatment is the extension of the Langmuir equation by Markham and Benton [29], who neglect interactions and assume that the only effect is the reduction of the vacant surface area for the adsorption of A because of adsorption of other components. For a binary gas mixture of A and B, let  $\theta_A$  = fraction of surface covered by A and  $\theta_B$  = fraction of surface covered by B. Then,  $(1 - \theta_A - \theta_B)$  = fraction of vacant surface. At equilibrium:

$$(k_A)_a p_A (1 - \theta_A - \theta_B) = (k_A)_d \theta_A \quad (15-28)$$

$$(k_B)_a p_B (1 - \theta_A - \theta_B) = (k_B)_d \theta_B \quad (15-29)$$

Solving these equations simultaneously, and combining results with (15-23), gives

$$q_A = \frac{(q_A)_m K_A p_A}{1 + K_A p_A + K_B p_B} \quad (15-30)$$

$$q_B = \frac{(q_B)_m K_B p_B}{1 + K_A p_A + K_B p_B} \quad (15-31)$$

where  $(q_i)_m$  is the maximum amount of adsorption of species  $i$  for coverage of the entire surface. Equations (15-30) and (15-31) are readily extended to a mixture of  $j$  components:

$$q_i = \frac{(q_i)_m K_i p_i}{1 + \sum_j K_j p_j} \quad (15-32)$$

In a similar fashion, as shown by Yon and Turnock [30], the Freundlich and Langmuir equations can be combined to give the following extended relation for gas mixtures:

$$q_i = \frac{(q_i)_0 k_i p_i^{1/n_i}}{1 + \sum_j k_j p_j^{1/n_j}} \quad (15-33)$$

where  $(q_i)_0$  is the maximum loading, which may differ from  $(q_i)_m$  for a monolayer. Equation (15-33) represents data for nonpolar, multicomponent mixtures in molecular sieves reasonably well. Broughton [31] has shown that both the extended-Langmuir and Langmuir–Freundlich equations lack thermodynamic consistency. Therefore, (15-32) and (15-33) are frequently referred to as nonstoichiometric isotherms. Nevertheless, for practical purposes, their simplicity often makes them the isotherms of choice.

Both (15-32) and (15-33) are also referred to as *constant-selectivity equilibrium* equations because they predict a separation factor (selectivity),  $\alpha_{i,j}$ , for each pair of components,  $i$ ,  $j$ , in a mixture that is constant for a given temperature and independent of mixture composition. For example, (15-32) gives

$$\alpha_{i,j} = \frac{q_i/q_j}{p_i/p_j} = \frac{(q_i)_m K_i}{(q_j)_m K_j}$$

As with vapor–liquid and liquid–liquid phase equilibria for three or more components, data for binary and multicomponent gas–solid adsorbent equilibria are scarce and less accurate than corresponding pure-gas data. Valenzuela and Myers [23] include experimental data on adsorption of gas mixtures from 9 published studies on 29 binary systems, for which pure-gas-adsorption isotherms were also obtained. They also describe procedures for applying the Toth and UNILAN equations to multicomponent mixtures based on the ideal-adsorbed-solution (IAS) theory of Myers and Prausnitz [32]. Unlike the extended-Langmuir equation (15-32), which is explicit in the amount adsorbed, the IAS theory, though more accurate, is not explicit and requires an iterative solution procedure. Additional experimental data for higher-order (ternary and/or higher) gas mixtures are given by Miller, Knaebel, and Ikels [33] for 5A molecular sieves and by Ritter and Yang [34] for activated carbon. Yang [25] presents a discussion of mixture adsorption theories, together with comparisons of these theories with mixture data for activated carbon and zeolites. The data on zeolites are the most difficult to correlate, with the statistical thermodynamic model (SSTM) of Ruthven and Wong [35] giving the best results.

#### EXAMPLE 15.5 Extended-Langmuir Isotherm.

The experimental work of Ritter and Yang, cited in Example 15.4, also includes adsorption isotherms for pure CO and CH<sub>4</sub>, and a binary mixture of CH<sub>4</sub> (A) and CO (B). Ritter and Yang give the following Langmuir constants for pure A and B at 294 K:

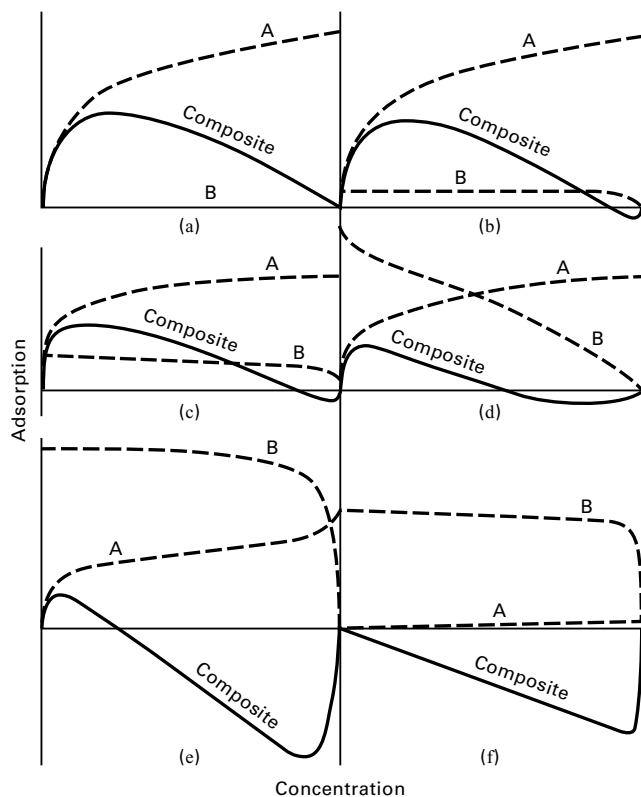


**Figure 15.13** Origin of various types of composite isotherms for binary-liquid adsorption.

[From J.J. Kipling, *Adsorption from Solutions of Non-electrolytes*, Academic Press, London (1965) with permission.]

It is then common to fit the data with concentration forms of the Freundlich (15-19) or Langmuir (15-24) equations:

$$q = kc^{1/n} \quad (15-35)$$

$$q = \frac{Kq_m c}{1 + Kc} \quad (15-36)$$

Candidate systems for this case are small amounts of organics dissolved in water and small amounts of water dissolved in hydrocarbons. For liquid mixtures dilute in two or more solutes, multicomponent adsorption may be estimated from a concentration form of the extended-Langmuir equation (15-32) based on constants,  $q_m$  and  $K$ , obtained from experiments on single solutes. However, when solute-solute interactions are suspected, it may be necessary to determine constants from multicomponent data. As with gas mixtures, the concentration form of (15-32) also predicts constant selectivity for each pair of components in a mixture.

#### EXAMPLE 15.6 Adsorption of VOCs.

Small amounts of VOCs in water can be removed by adsorption. Generally, two or more VOCs are present. An aqueous stream containing small amounts of acetone (1) and propionitrile (2) is to be treated with activated carbon. Single-solute equilibrium data from

Radke and Prausnitz [37] have been fitted to the Freundlich and Langmuir isotherms, (15-35) and (15-36), with the average deviations indicated, for solute concentrations up to 50 mmol/L:

Acetone in Water (25°C):		Absolute Average Deviation of $q$ , %
$q_1 = 0.141c_1^{0.597}$	(1)	14.2
$q_1 = \frac{0.190c_1}{1 + 0.146c_1}$	(2)	27.3
Propionitrile in water (25°C):		
$q_2 = 0.138c_2^{0.658}$	(3)	10.2
$q_2 = \frac{0.173c_2}{1 + 0.0961c_2}$	(4)	26.2

where  $q_i$  = amount of solute adsorbed, mmol/g, and  $c_i$  = solute concentration in aqueous solution, mmol/L.

Use these single-solute results with an extended Langmuir-type isotherm to predict the equilibrium adsorption in a binary-solute, aqueous system containing 40 and 34.4 mmol/L, respectively, of acetone and propionitrile at 25°C with the same adsorbent. Compare the results with the following experimental values from Radke and Prausnitz [37]:

$$q_1 = 0.715 \text{ mmol/g}, q_2 = 0.822 \text{ mmol/g}, \text{ and } q_{\text{total}} = 1.537 \text{ mmol/g}$$

#### Solution

From (15-32), the extended liquid-phase Langmuir isotherm is

$$q_i = \frac{(q_i)_m K_i c_i}{1 + \sum_j K_j c_j} \quad (5)$$

From (2),  $(q_1)_m = 0.190/0.146 = 1.301$  mmol/g.

From (4),  $(q_2)_m = 0.173/0.0961 = 1.800$  mmol/g.

From (5):

$$q_1 = \frac{1.301(0.146)(40)}{1 + (0.146)(40) + (0.0961)(34.4)} = 0.749 \text{ mmol/g}$$

$$q_2 = \frac{1.800(0.0961)(34.4)}{1 + (0.146)(40) + (0.0961)(34.4)} = 0.587 \text{ mmol/g}$$

Summing,  $q_{\text{total}} = 1.336$  mmol/g.

Compared to experimental data, the percent deviations for  $q_1$ ,  $q_2$ , and  $q_{\text{total}}$ , respectively, are 4.8%, -28.6%, and -13.1%. Better agreement is obtained by Radke and Prausnitz using an IAS theory. It is expected that a concentration form of (15-33) would also give better agreement, but that requires that the single-solute data be refitted for each solute to a Langmuir-Freundlich isotherm of the form

$$q = \frac{q_0 kc^{1/n}}{1 + kc^{1/n}} \quad (6)$$

#### §15.2.4 Ion-Exchange Equilibria

Ion exchange differs from adsorption in that one sorbate (a counterion) is exchanged for a solute ion, the process being governed by a reversible, stoichiometric, chemical-reaction

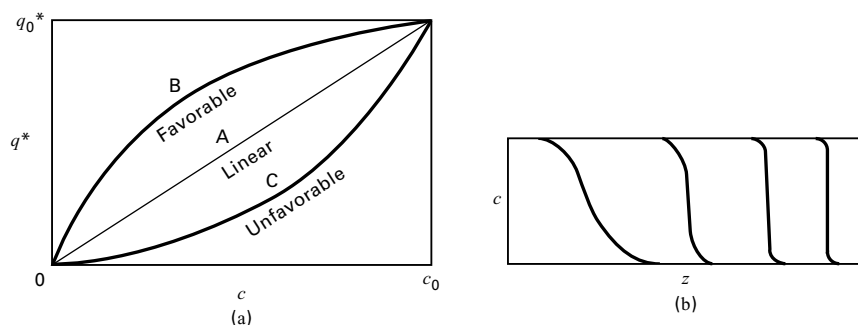


**Figure 15.34** Effect of shape of isotherm on sharpness of concentration wave front. (a) Isotherm shapes. (b) Self-sharpening wave front caused by a favorable adsorption isotherm.

### Scale-Up Using Constant-Pattern Front

Persistent transport-rate resistance eventually limits self-sharpening, and an asymptotic or *constant-pattern front* (CPF) is developed. For such a front, MTZ becomes constant and curves of  $c_f/c_F$  and  $\bar{c}_b/\bar{c}_b^*$  become coincident. The bed depth at which CPF is approached depends upon the non-linearity of the adsorption isotherm and the importance of adsorption kinetics. Cooney and Lightfoot [130] proved the existence of an asymptotic wave-front solution, including effects of axial dispersion. Initially, the wave front broadens because of mass-transfer resistance and/or axial dispersion. Analytical solutions for CPF from Sircar and Kumar [131] and a rapid approximate method based on Freundlich and Langmuir isotherms from Cooney [132] are available to estimate CPF concentration profiles and breakthrough curves using mass-transfer and equilibrium parameters.

When the constant-pattern-front assumption is valid, it can be used to determine the length of a full-scale adsorbent bed from breakthrough curves obtained in small-scale laboratory experiments. This widely used technique is described by Collins [133] for purification applications.

Total bed length is taken to be

$$L_B = \text{LES} + \text{LUB} \quad (15-86)$$

the sum of the length of an ideal, equilibrium-adsorption section, LES, unaffected by mass-transfer resistance

$$\text{LES} = \frac{c_F Q_F t_b}{q_F \rho_b A} \quad (15-87)$$

where  $Q_F$  is the volumetric feed flow rate, plus a length of unused bed, LUB, determined by the MTZ width and the  $c_f/c_F$  profile within that zone, using

$$\text{LUB} = \frac{L_e}{t_s} (t_s - t_b) \quad (15-88)$$

where  $L_e/t_s$  is the ideal wave-front velocity. The stoichiometric time  $t_s$  divides the MTZ (e.g., CPF zone) into equal areas A and B as shown in Figure 15.35, and  $L_e/t_s$  corresponds to the ideal wave-front velocity. Alternatively,  $t_s$  may be determined using

$$t_s = \int_0^{t_e} \left( 1 - \frac{c_f}{c_F} \right) dt \quad (15-89)$$

For example, if  $t_s$  equalizes areas A and B when it is equidistant between  $t_b$  and  $t_e$ , then  $\text{LUB} = \text{MTZ}/2$ . A conservative estimate of MTZ = 4 ft may be used in the absence of experimental data.

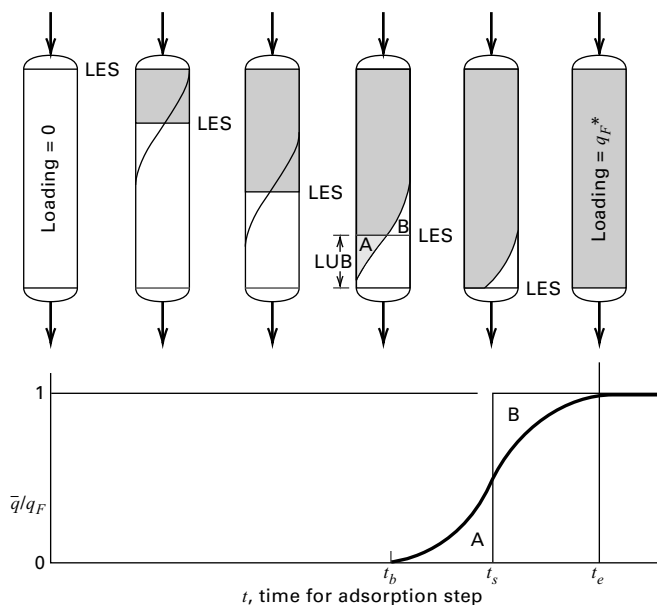


**Figure 15.35** Determination of bed length from laboratory measurements.

### EXAMPLE 15.14 Scale-Up for Fixed-Bed Adsorption.

Collins [133] reports the experimental data below for water-vapor adsorption from nitrogen in a fixed bed of 4A molecular sieves for bed depth = 0.88 ft, temperature = 83°F, pressure = 86 psia,  $G$  = entering gas molar velocity = 29.6 lbmol/h-ft<sup>2</sup>, entering water content = 1,440 ppm (by volume), initial adsorbent loading = 1 lb/100 lb sieves, and bulk density of bed = 44.5 lb/ft<sup>3</sup>. For the entering gas moisture content,  $c_F$ , the equilibrium loading,  $q_F$ , = 0.186 lb H<sub>2</sub>O/lb solid.

$c_{\text{exit}}$ , ppm (by volume)	Time, h	$c_{\text{exit}}$ , ppm (by volume)	Time, h
<1	0–9.0	650	10.8
1	9.0	808	11.0
4	9.2	980	11.25
9	9.4	1,115	11.5
33	9.6	1,235	11.75
80	9.8	1,330	12.0
142	10.0	1,410	12.5
238	10.2	1,440	12.8
365	10.4	1,440	13.0
498	10.6		

Determine the bed height required for a commercial unit to be operated at the same temperature, pressure, and entering gas mass velocity and water content to obtain an exiting gas with no more than 9 ppm (by volume) of water vapor with a breakthrough time of 20 h.

### Solution

$$c_F = \frac{1,440(18)}{106} = 0.02592 \text{ lb H}_2\text{O/lbmol N}_2$$

$$G = \frac{Q_F}{\pi D^2/4} = 29.6 \text{ lbmol N}_2/\text{h-ft}^2 \text{ of bed cross-section}$$

Initial moisture content of bed = 0.01 lb H<sub>2</sub>O/lb solid

From (15-87), revised for a gas flow rate based on the lbmol of N<sub>2</sub> instead of the volume in ft<sup>3</sup> of N<sub>2</sub>,

$$\text{LES} = \frac{(0.02592)(29.6)(20)}{(0.186 - 0.01)(44.5)} = 1.96 \text{ ft}$$

Use the integration method to obtain LUB. From the data:

Take  $t_e = 12.8$  h (1,440 ppm) and  $t_b = 9.4$  h (9 ppm).

By numerical integration of breakthrough-curve data, using (15-88):  $t_s = 10.93$  h.

From (15-88),

$$\text{LUB} = \left( \frac{10.93 - 9.40}{10.93} \right) (0.88) = 0.12 \text{ ft}$$

From (15-86),  $L_B = 1.96 + 0.12 = 2.08$  ft, or a bed utilization of  $\frac{1.96}{2.08} \times 100\% = 94.2\%$ .

Alternatively, an approximate calculation can be made. Let  $t_b$ , the beginning of breakthrough, be 5% of the final ppm, or 0.05 (1,440) = 72 ppm. Using the experimental data, this corresponds to  $t_b = 9.76$  h. Let  $t_e$ , the end of breakthrough, be 95% of the final ppm, or 0.95(1,440) = 1,370 ppm, corresponding to  $t_e = 12.25$  h.

Let  $t_s$  = the midpoint or  $(9.76 + 12.25)/2 = 11$  h. The ideal wave-front velocity =  $L_e/t_s = 0.88/11 = 0.08$  ft/h. From (15-87),  $\text{LUB} = 0.08(11 - 9.76) = 0.1$  ft.  $\text{MTZ} = 0.2$  ft and  $L_B = 1.96 + 0.1 = 2.06$  ft.

### §15.3.6 Multicomponent Differential Chromatography

Most separation systems discussed thus far perform a binary split between key components (e.g., LK and HK in distillation). Chromatography can separate multicomponent mixtures into 2+ products, whose elution time,  $t = z_L/f_s u$ , increases proportionally to relative thermodynamic partitioning of each species from moving fluid to stationary adsorptive phase (15-51). Transport-rate processes (e.g., 15-57 and 15-58) dilute the product concentration and mix adjacent solutes. Figure 15.36 illustrates differential chromatography, also called batch or elution chromatography, in which a feed mixture insufficient to load the sorbent is pulsed into the feed end of the column.

An eluant carrier gas or solvent moving at a constant plug-flow interstitial velocity  $u$  that has little or no affinity for the sorbent moves the fraction of solute desorbed into the fluid phase (15-54) along the length of the column at solute wave (migration) velocity  $u_c = \omega u$ , given in (15-85), as solute readsorbs and desorbs in succession via mass action. Transport-rate processes broaden each solute peak as it proceeds along the column. The solute migration velocity, given by (15-85), is smaller for solutes with higher affinity, i.e., smaller  $\alpha$  corresponding to a larger  $K_d$  in (15-51). Initially, overlapping solute peaks are gradually separated by the fractional difference in migration velocities of adjacent, noninteracting

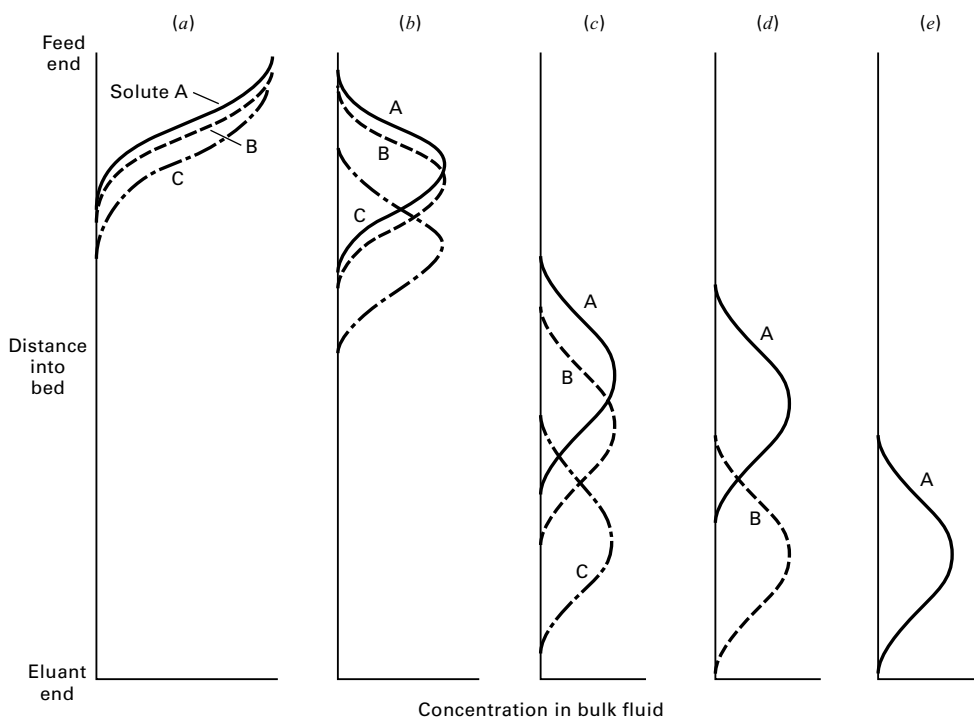


**Figure 15.36** Movement of concentration waves during separation in a chromatographic column.